Supplementary Information to “Reduction of apparent temporal variations of tidal parameters by a proper local response model”

Adam Ciesielski [1,3*], Thomas Forbriger [1,2], Walter Zürn [1,2] and Andreas Rietbrock [1]

[1*]Geophysical Institute (GPI), Karlsruhe Institute of Technology (KIT), Hertzstraße 16, 76187 Karlsruhe, Germany.

[2]Black Forest Observatory (Schiltach), Karlsruhe Institute of Technology and University of Stuttgart, Heubach 206, 77709 Wolfach, Germany.

[3]Geodetic Institute (GIK), Karlsruhe Institute of Technology (KIT), Englerstraße 7, 76131 Karlsruhe, Germany.

*Corresponding author(s). E-mail(s): adam.ciesielski@kit.edu;
Contributing authors: thomas.forbriger@kit.edu; walter.zuern@partner.kit.edu; andreas.rietbrock@kit.edu;

1 Tables

1.1 Names of waves

In all recent works on tidal analysis, the researchers define different names for the newly identified waves, which could lead to confusion. Therefore, we present a comparison of different naming conventions. Tables S1-S3 list names attributed to significant tides distinguished by this work (Tab. B1-B4 from the main paper), Bartels (1957, Table 2.), Melchior et al (1996, Table 5.) and Calvo (2015, Tables 5.2-5.5). To avoid confusion, we provide the corresponding Doodson number to each wave. Bartels (1957) identifies some significant waves, giving no name, which is described with the ellipsis (...). In this work, we only allow for 1-digit subscripts at the end as an indication of tidal species to avoid confusions while applying the wave name into the tidal catalog file. Waves with ‡ in the first columns are harmonics that we initially used for reference groups in the analysis, but later we have not found them significant. They are missing in Tables B1-B4 for this reason.

2 Figures

2.1 The moving window analysis (MWA)

Figures S1 - S3 display results of the moving window analysis for all twelve wave groups. This is an extension of Figure 7 from the manuscript. As expected, temporal variations are smaller after the local response model was used as the a priori model. However, for some groups the difference does not appear significant.

Ciesielski	Melchior	Calvo	Bartels	Doodson
ζ_1		1158		115.855
SGQ_1	SGQ_1	SGQ_1		117.655
		$\mathrm{2Q}_{1\mathrm{x}}$		125.745
$\mathrm{2Q}_1$	$2Q_1$	$\mathrm{2Q}_1$	$\mathbf{2Q}_1$	125.755
		$\mathrm{SGM}_{1\mathrm{x}}$		127.545
σ_1	Sig_1	SGM_1	σ_1	127.555
o_1		$\mathrm{Q}_{1\mathrm{x}}$	...	135.645
Q_1	Q_1	Q_1	$\mathbf{Q}_1$	135.655
ρ_1	RO_1	RO_1	ρ_1	137.455
		$\mathrm{O}_{1\mathrm{x}}$	...	145.545
O_1	O_1	O_1	$\mathbf{O}_1$	145.555
		$\mathrm{2NO}_1$		145.755
τ_1	Tau_1	TAU_1	τ_1	147.555
		NTAU		153.655
		$\mathrm{LK}_{1\mathrm{x}}$		155.445
LK_1	LK_1	LK_1	...	155.455
M_1	NO_1	NO_1	$\mathbf{M}_1$	155.655
‡MN_1		$\mathrm{NO}_{1\mathrm{x}}$		155.665
χ_1	Chi_1	CHI_1	χ_1	157.455
π_1	Pi_1	PI_1	π_1	162.556
		$\mathrm{P}_{1\mathrm{x}}$		163.545
P_1	P_1	P_1	$\mathbf{P}_1$	163.555
S_1	S_1	S_1	$\mathbf{S}_1$	164.556
		K_{1x-}		165.545
K_1	K_1	K_1	$\mathbf{K}_1$	165.555
κ_1		K_{1x+}	...	165.565
ψ_1	Psi_1	PSI_1	ψ_1	166.554
φ_1	Phi_1	PHI_1	φ_1	167.555
ϑ_1	TET_1	TET_1	ϑ_1	173.655
J_1	J_1	J_1	$\mathbf{J}_1$	175.455
ι_1		$\mathrm{J}_{1\mathrm{x}}$		175.465
SO_1	SO_1	SO_1	$\mathbf{SO}_1$	183.555
		$\mathrm{2J}_1$		185.355
OO_1	OO_1	OO_1	$\mathbf{OO}_1$	185.555
		$\mathrm{OO}_{1\mathrm{x}}$	...	185.565
V_1	Nu_1	NU_1	υ_1	195.455
		$\mathrm{NU}_{1\mathrm{x}}$		195.465

Table S1: Names of diurnal degree 2 tides used by different authors (Bartels, 1957; Melchior et al, 1996; Calvo, 2015).

Ciesielski	Melchior	Calvo	Bartels	Doodson
$\mathrm{3N}_2$	$3N_2$	$\mathrm{3N}_2$	$\mathbf{3N}_2$	225.855
ϵ_2	Eps_2	EPS_2	ϵ_2	227.655
$\mathrm{2N}_2$	$2N_2$	$\mathrm{2N}_2$	$\mathbf{2N}_2$	235.755
μ_2	Mu_2	MU_2	μ_2	237.555
		$\mathrm{N}_{2\mathrm{x}}$		245.645
N_2	N_2	N_2	$\mathbf{N}_2$	245.655
ν_2	Nu_2	NU_2	ν_2	247.455
γ_2		GAM_2	γ_2	253.755
α_2		ALF_2	α_2	254.556
ω_2		$\mathrm{M}_{2\mathrm{x}}$	...	255.545
M_2	M_2	M_2	$\mathbf{M}_2$	255.555
β_2		BET_2	β_2	256.554
δ_2		DEL_2	δ_2	257.555
λ_2	Lam_2	LAM_2	λ_2	263.655
L_2	L_2	L_2	$\mathbf{L}_2$	265.455
‡KNO_2	KNO_2	KNO_2	...	265.655
			$\mathbf{2T}_2$	271.557
T_2	T_2	T_2	$\mathbf{T}_2$	272.556
S_2	S_2	S_2	$\mathbf{S}_2$	273.555
R_2	R_2	R_2	$\mathbf{R}_2$	274.554
K_2	K_2	K_2	$\mathbf{K}_2$	275.555
		$\mathrm{K}_{2\mathrm{x}}$	...	275.565
‡ζ_2		ZET_2	ζ_2	283.655
η_2	Eta_2	ETA_2	$\eta 2$	285.455
		ETA_x		285.465
$\mathrm{2S}_2$	$2S_2$	$\mathrm{2S}_2$		293.555
$\mathrm{2K}_2$	$2K_2$	$\mathrm{2K}_2$	...	295.555

Table S2: Names of semi-diurnal degree 2 tides used by different authors (Bartels, 1957; Melchior et al, 1996; Calvo, 2015).

2.2 Histograms of moving window analysis

We analyzed the distribution of parameter values in moving window analysis, using WDZe and BF21 as a priori model. As clearly seen in Figs. S4 - S6 the distribution is more reasonable, Gaussian, if the correction was applied. The distribution that does not meet the expectation, i.e. is rather uniform than normal, has high skewness or appears as a sum of two Gaussians, is most visible without the local response a priori model in groups K_1, N_2 or L_2, both factor and phase. In fact, the small improvement in terms of narrowing the distribution is even noticeable for M_2, which was not that clear if only time series were analyzed.

2.3 Spectra of moving window analysis

Wy apply a Fourier transformation to the parameter time series obtained by MWA as displayed in Fig. S1 - S3. The Fourier amplitude spectra are displayed in Fig. S7 - S9. The MWA results were not tapered for the purpose of this analysis. Linear trends were subtracted before applying the Fourier transformation. The systematic peaks or periodic counterpart visible in the spectra vanish if proper local response model BF21 is applied. Groups K_1, μ_2 and N_2 serve as good examples. In addition, not only periodic, but strange patterns in M_1 or J_1 were not present when the local response model

Ciesielski	Melchior	Calvo	Bartels	Doodson
o_1*	$3MK_1$	$3MK_1$		135.555
O_1*				145.655
M_1*	M_1	M_1		155.555
ι_1*	$3MO_1$	$3MO_1$		175.555
$3N_2$*				225.755
$2N_2$*	$3MJ_2$	$3MJ_2$		235.655
		$3MK_x$		237.455
N_2*	$3MK_2$	$3MK_2$	…	245.555
M_2*				255.655
L_2*	$3MO_2$	$3MO_2$	…	265.555
		$3MO_x$		265.565
		$3MQ_2$		273.655
K_2*		$3KM_2$		275.455
MN_3*	MN_3	MN_3	…	345.655
		M_{3x}		355.545
M_3*	M_3	M_3	$\mathbf{M_3}$	355.555
ML_3*	ML_3	ML_3		365.455
MK_3*	MK_3	MK_3		375.555
		N_4		435.755
M_4+		M_4		455.555
		K_4		475.565

Table S3: Names of degree 3 and 4 tides used by different authors (Bartels, 1957; Melchior et al, 1996; Calvo, 2015).

was used. The units on the y-axis are arbitrary units (a.u.).

2.4 MWA of air pressure and misfit

Figures S10 display the results of moving window analysis for air pressure factor and data misfit. The expectation is that the variation in air pressure coefficient should not be strongly altered in these two approaches, as seen in the figures. In addition, the data misfit (tapered and untapered) should be in general slightly smaller with the BF21˙This is also demonstrated by the plots. There are few cases where misfit increases if the BF21 is used. Dashed lines provide values that are results from the analysis of the full time series.

3 RATA method

The steps described in sections 2. and 4. were visualised and some technical specifications were provided. The concept of the iterative procedure is presented in the Fig. S11.

4 Animations demonstrating regularization method

We prepared gif files (also with pdf version) that visualize the trade-off problem, so how the values $\vec{m}(\alpha)$ as tidal parameters (δ, Φ) change for different α, with indication of the point on the $\Delta_\mathrm{d}(\alpha) - \Delta_\mathrm{m}(\alpha)$ misfit curve. This is the presentation of Figs. 1-3 (main paper), extended. Three different movies correspond to three different iterations, are in files:

- Initial iteration: `FrequencySpectra0`
- First iteration: `FrequencySpectra1`
- Final iteration: `FrequencySpectra4`

In the animations panels indicate: gravimetric factor estimates δ (left top), gravimetric phase estimates Φ (left bottom), misfit curves (right top) and spectra of the data misfit (right bottom).

- Initial iteration: `AmplitudeTimeSeries0`
- First iteration: `AmplitudeTimeSeries1`
- Final iteration: `AmplitudeTimeSeries4`

In each animation panels indicate: $(\vec{m} - \vec{m}^\mathrm{ref})$ for in phase adjustments x (left top) and quadrature adjustments y (left bottom), as a function of acceleration amplitude, misfit curves (right top) and residual time series (right bottom).

At the final iteration, no reference model update was performed. Even though there is an indication that 1-3 significant harmonics deviate at particular value of data misfit (corresponding to previous trade-off points), we could not localize any trace of distinctive change of the misfit curve shape there. Thus, the reference model in this iteration is the final local response model.

References

Bartels J (1957) Gezeitenkräfte [Tidal Forces]. In: Flügge S (ed) Handbuch der Physik, vol 48: Geophysik: 2. Springer, Berlin, https://doi.org/10.1017/9781316998793

Calvo M (2015) Analysis of long-term gravity records in europe: consequences for the retrieval of small amplitude and low frequency signals including the core resonance effects.

PhD thesis, Université de Strasbourg; Universidad complutense de Madrid, URL https://tel.archives-ouvertes.fr/tel-01222234

Melchior P, Ducarme B, Francis O (1996) The response of the Earth to tidal body forces described by second- and third-degree spherical harmonics as derived from a 12 year series of measurements with the superconducting gravimeter GWR/T3 in Brussels. Phys Earth Planet Inter 93(3–4):223–238. https://doi.org/10.1016/0031-9201(95)03073-5

Schroth E, Forbriger T, Westerhaus M (2018) A catalogue of gravimetric factor and phase variations for twelve wave groups. KIT scientific working papers 101. https://doi.org/10.5445/IR/1000089609

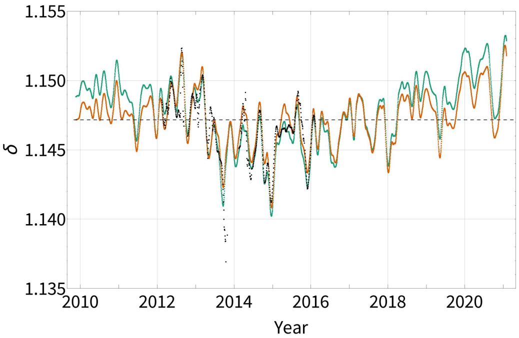

(a) Gravimetric factor of Q_1 tidal group

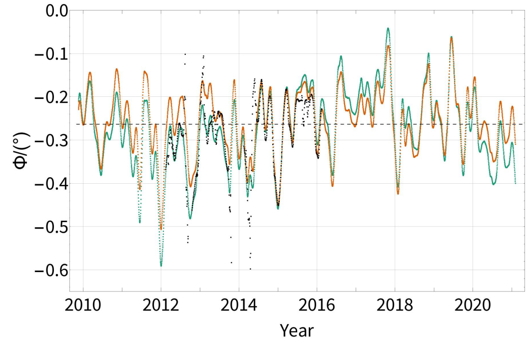

(b) Gravimetric phase of Q_1 tidal group

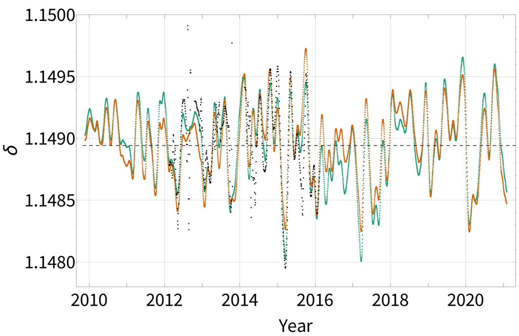

(c) Gravimetric factor of O_1 tidal group

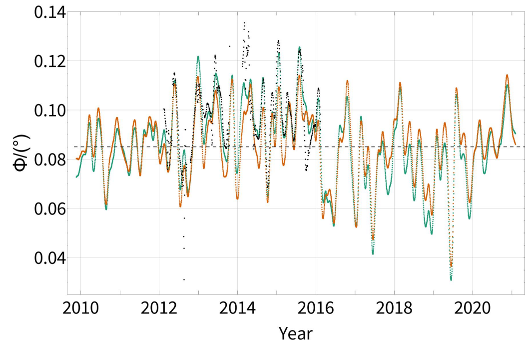

(d) Gravimetric phase of O_1 tidal group

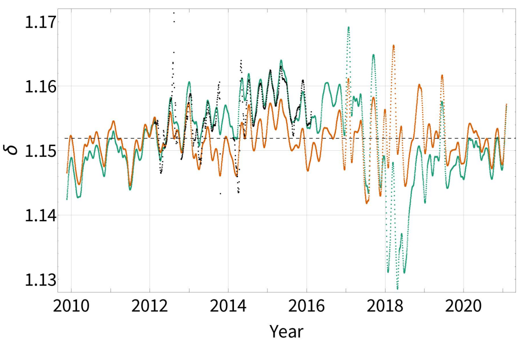

(e) Gravimetric factor of M_1 tidal group

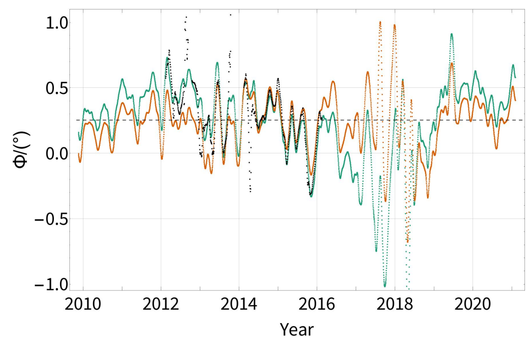

(f) Gravimetric phase of M_1 tidal group

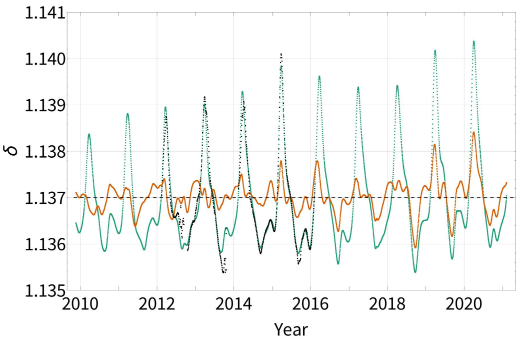

(g) Gravimetric factor of K_1 tidal group

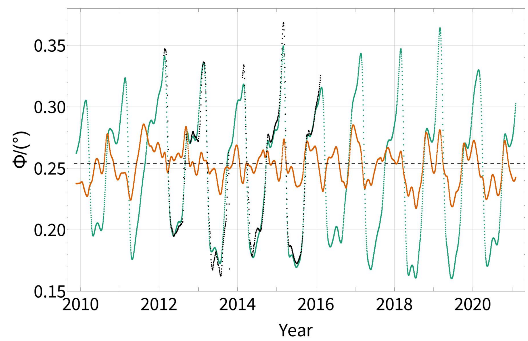

(h) Gravimetric phase of K_1 tidal group

Fig. S1: The results of moving window analysis for tidal groups Q_1, O_1, M_1 and K_1 (top to bottom) for gravimetric factor (left) and phase (right). Colors: green: MWA with a-priori WDZe-model, orange: MWA with a-priori BF21-model, black: results by Schroth et al (2018) for comparison.

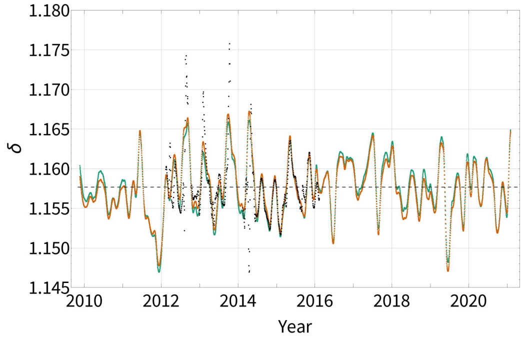

(a) Gravimetric factor of J_1 tidal group

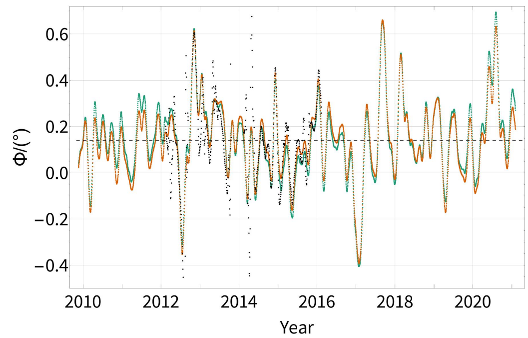

(b) Gravimetric phase of J_1 tidal group

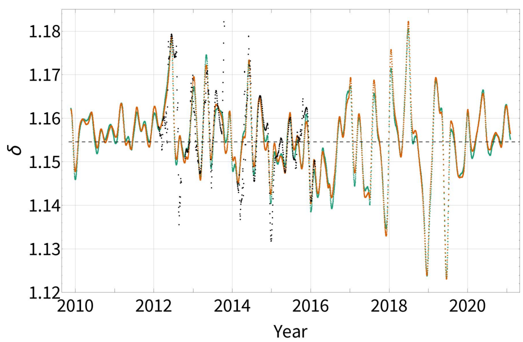

(c) Gravimetric factor of OO_1 tidal group

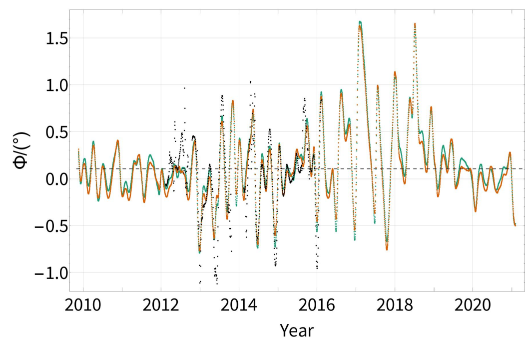

(d) Gravimetric phase of OO_1 tidal group

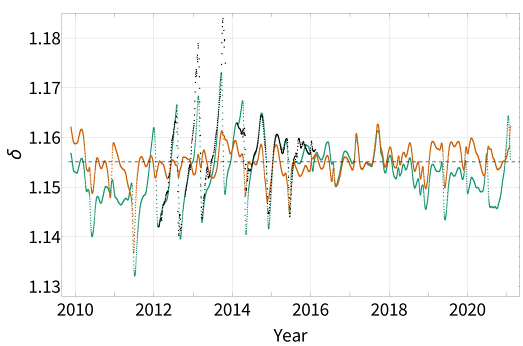

(e) Gravimetric factor of μ_2 tidal group

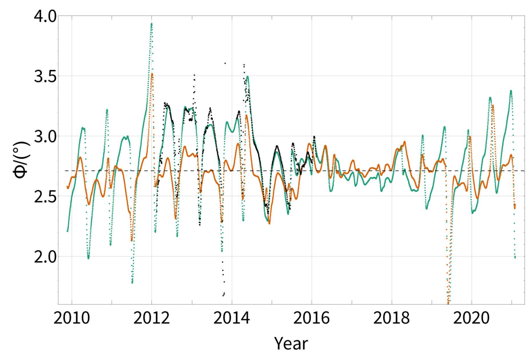

(f) Gravimetric phase of μ_2 tidal group

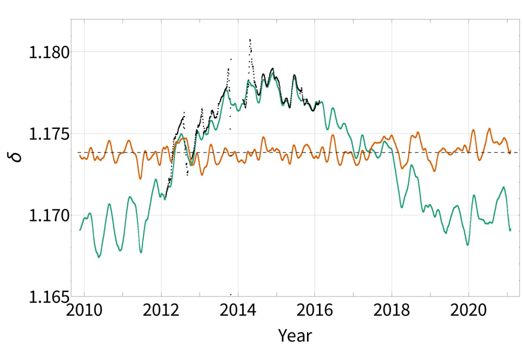

(g) Gravimetric factor of N_2 tidal group

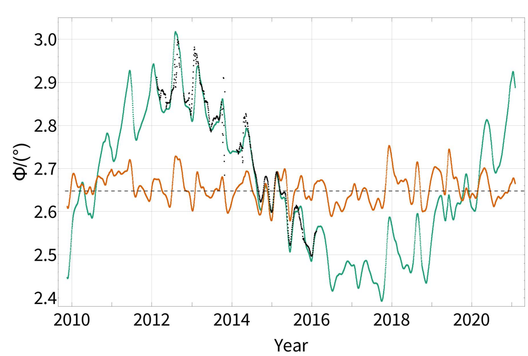

(h) Gravimetric phase of N_2 tidal group

Fig. S2: The results of moving window analysis for tidal groups J_1, OO_1, μ_2 and N_2 (top to bottom) for gravimetric factor (left) and phase (right). Colors: green: MWA with a-priori WDZe-model, orange: MWA with a-priori BF21-model, black: results by Schroth et al (2018) for comparison.

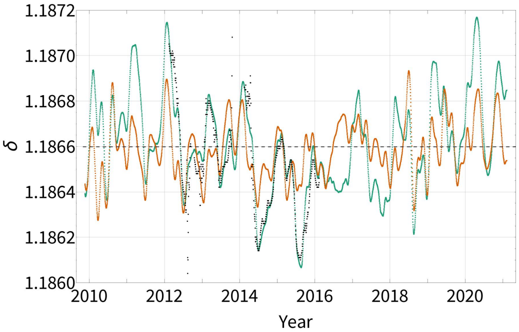

(a) Gravimetric factor of M_2 tidal group

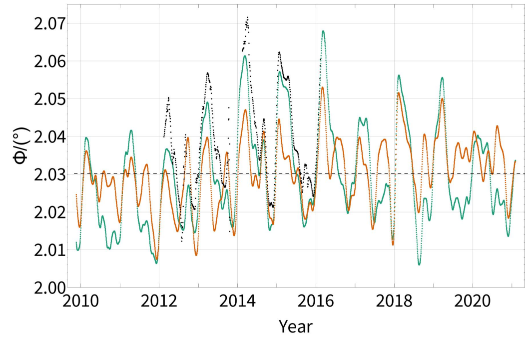

(b) Gravimetric phase of M_2 tidal group

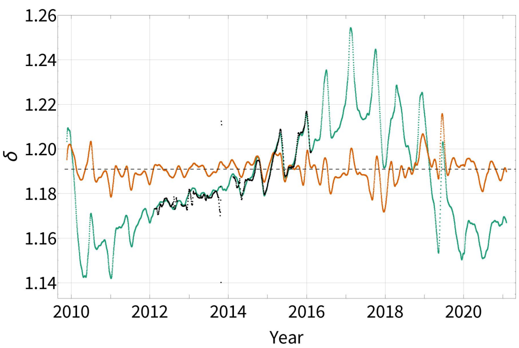

(c) Gravimetric factor of L_2 tidal group

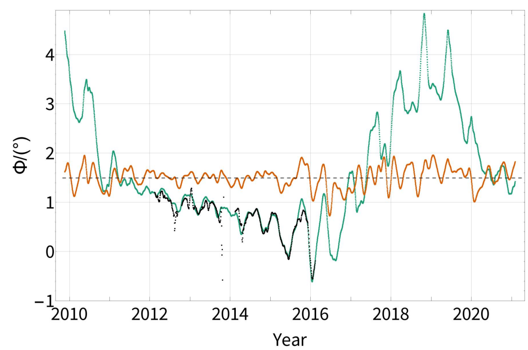

(d) Gravimetric phase of L_2 tidal group

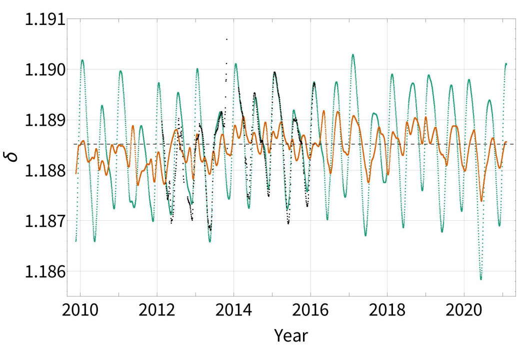

(e) Gravimetric factor of S_2 tidal group

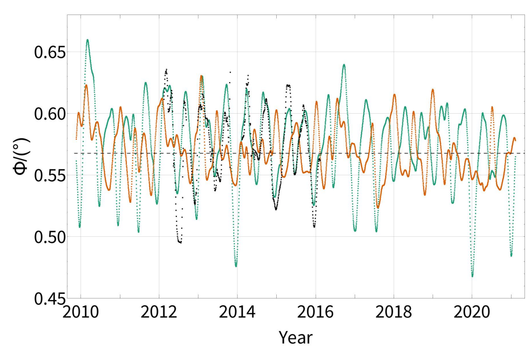

(f) Gravimetric phase of S_2 tidal group

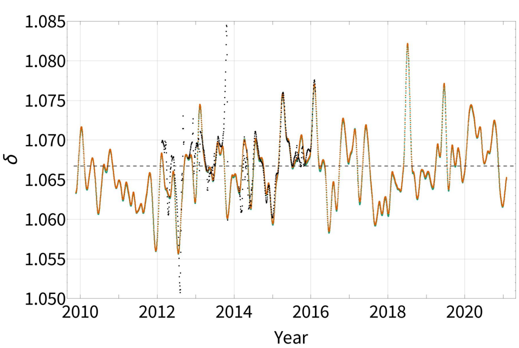

(g) Gravimetric factor of M_3* tidal group

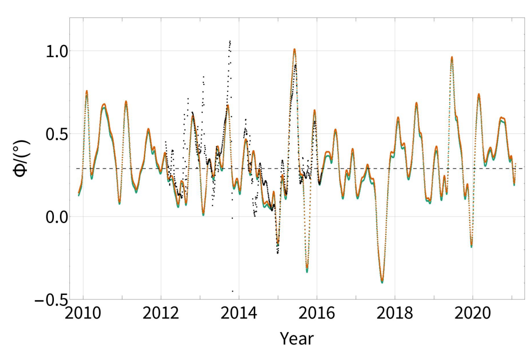

(h) Gravimetric phase of M_3* tidal group

Fig. S3: The results of moving window analysis for tidal groups M_2, L_2, S_2 and M_3* (top to bottom) for gravimetric factor (left) and phase (right). Colors: green: MWA with a-priori WDZe-model, orange: MWA with a-priori BF21-model, black: results by Schroth et al (2018) for comparison.

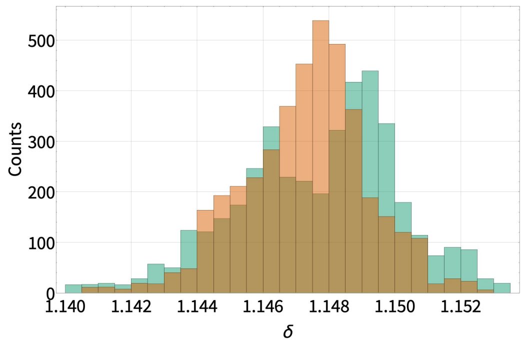

(a) Gravimetric factor of Q_1 tidal group

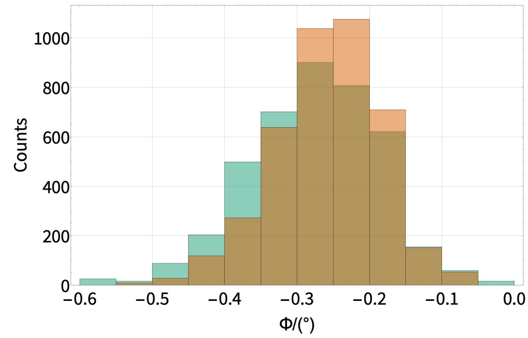

(b) Gravimetric phase of Q_1 tidal group

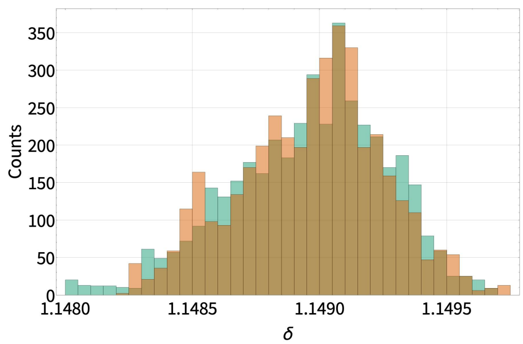

(c) Gravimetric factor of O_1 tidal group

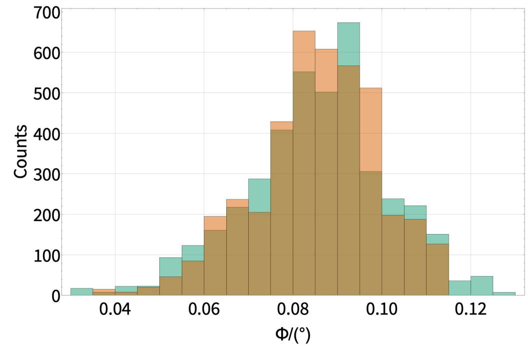

(d) Gravimetric phase of O_1 tidal group

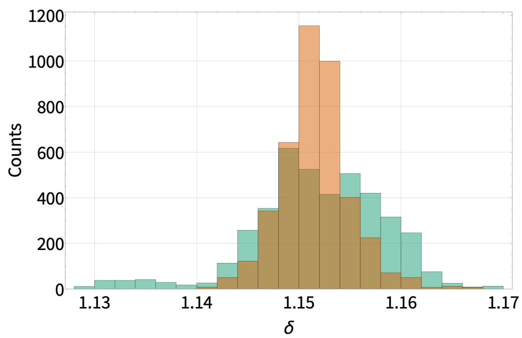

(e) Gravimetric factor of M_1 tidal group

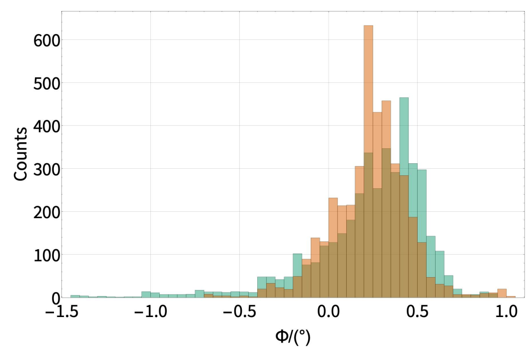

(f) Gravimetric phase of M_1 tidal group

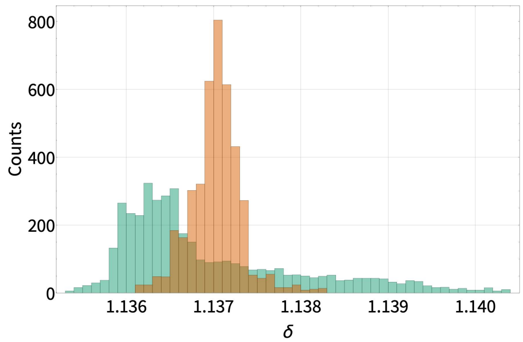

(g) Gravimetric factor of K_1 tidal group

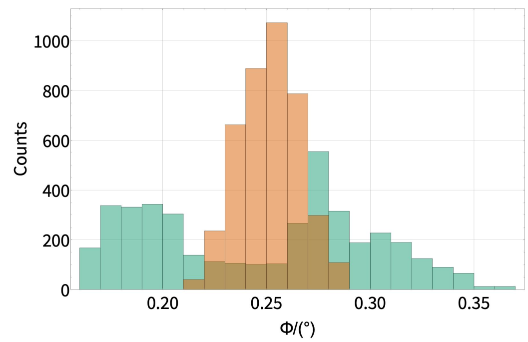

(h) Gravimetric phase of K_1 tidal group

Fig. S4: The histograms of moving window analysis for tidal groups Q_1, O_1, M_1 and K_1 (top to bottom) for gravimetric factor (left) and phase (right). Colors: green: MWA with a-priori WDZe-model, orange: MWA with a-priori BF21-model.

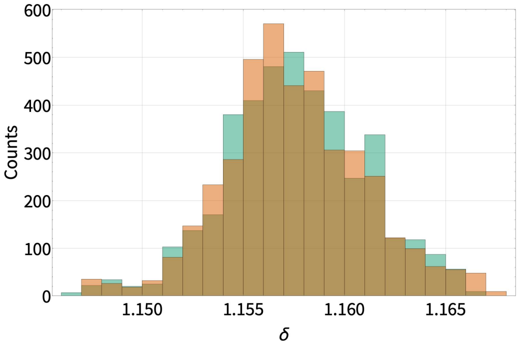

(a) Gravimetric factor of J_1 tidal group

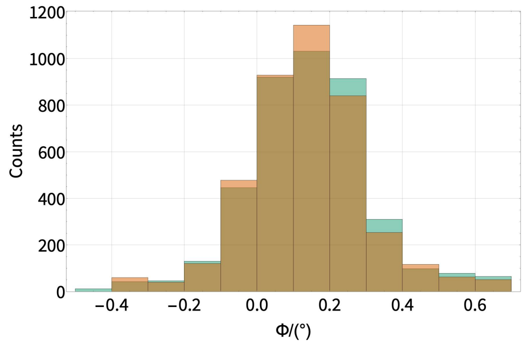

(b) Gravimetric phase of J_1 tidal group

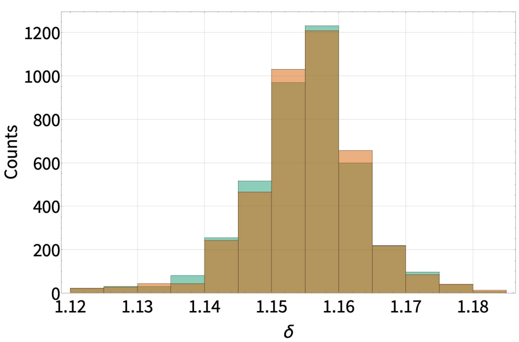

(c) Gravimetric factor of OO_1 tidal group

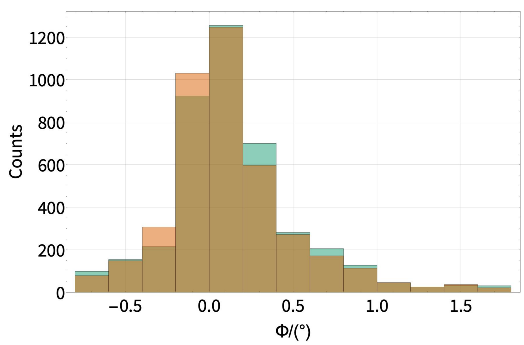

(d) Gravimetric phase of OO_1 tidal group

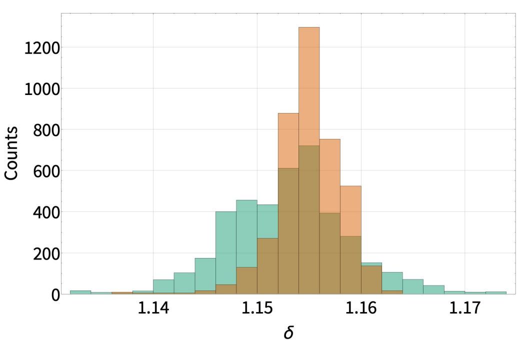

(e) Gravimetric factor of μ_2 tidal group

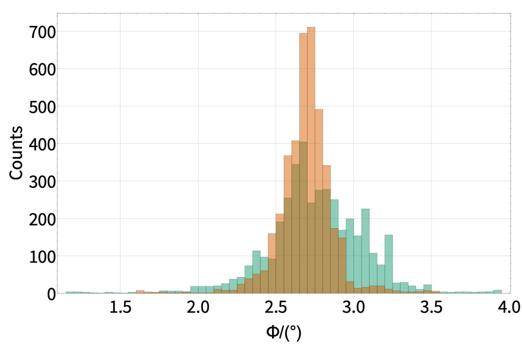

(f) Gravimetric phase of μ_2 tidal group

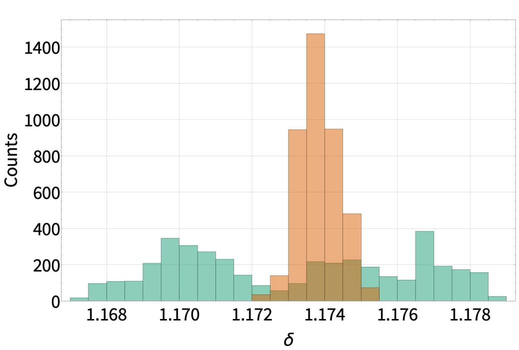

(g) Gravimetric factor of N_2 tidal group

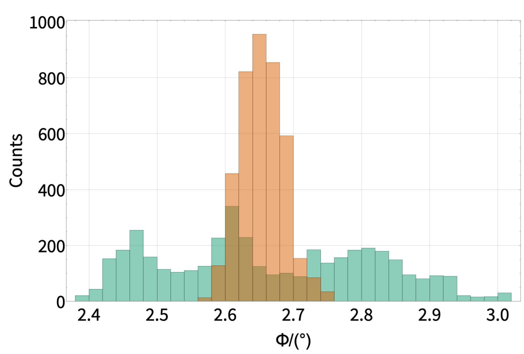

(h) Gravimetric phase of N_2 tidal group

Fig. S5: The histograms of moving window analysis for tidal groups J_1, OO_1, μ_2 and N_2 (top to bottom) for gravimetric factor (left) and phase (right). Colors: green: MWA with a-priori WDZe-model, orange: MWA with a-priori BF21-model.

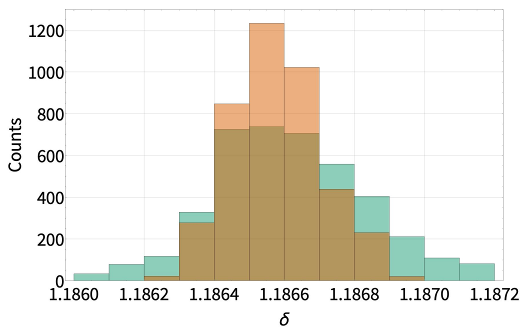

(a) Gravimetric factor of M_2 tidal group

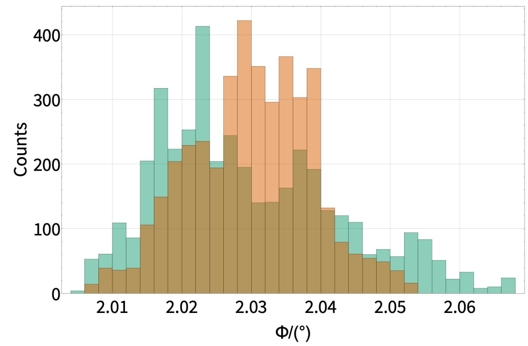

(b) Gravimetric phase of M_2 tidal group

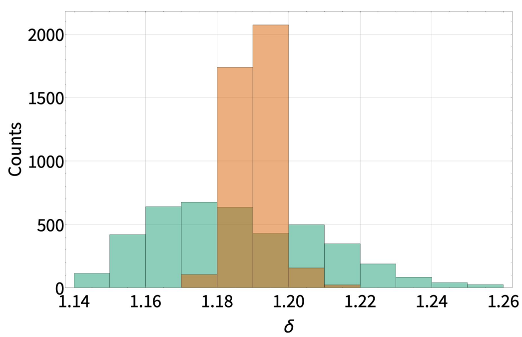

(c) Gravimetric factor of L_2 tidal group

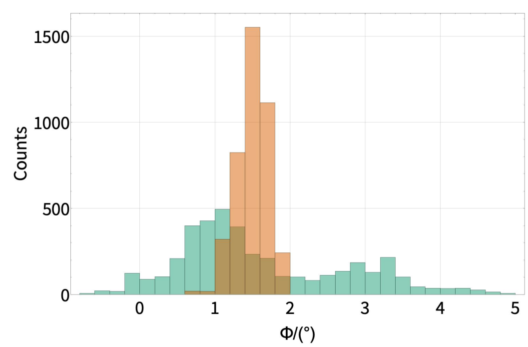

(d) Gravimetric phase of L_2 tidal group

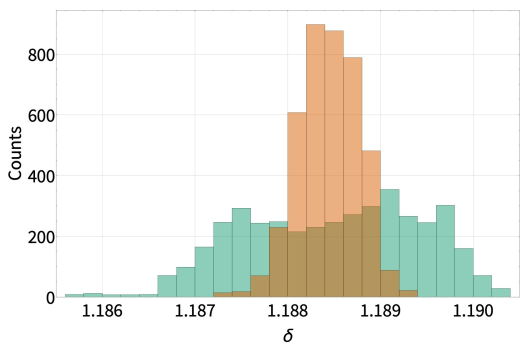

(e) Gravimetric factor of S_2 tidal group

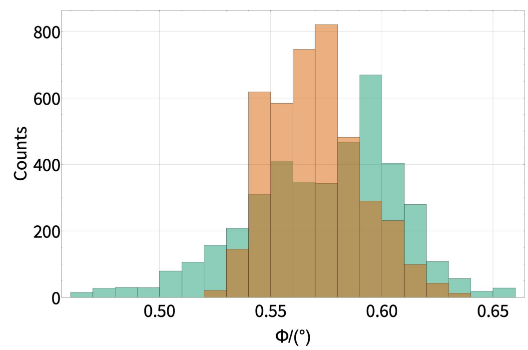

(f) Gravimetric phase of S_2 tidal group

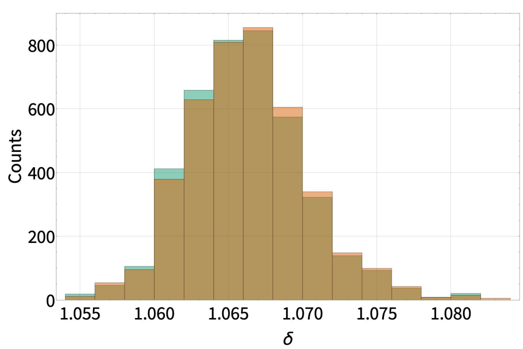

(g) Gravimetric factor of M_3* tidal group

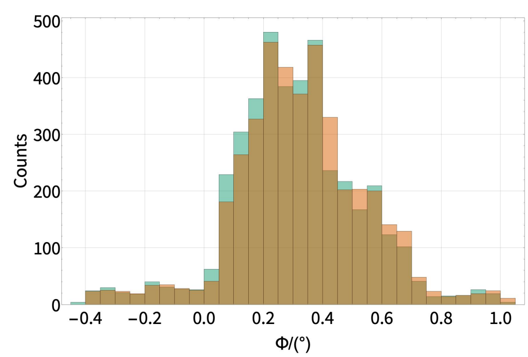

(h) Gravimetric phase of M_3* tidal group

Fig. S6: The histograms of moving window analysis for tidal groups M_2, L_2, S_2 and M_3* (top to bottom) for gravimetric factor (left) and phase (right). Colors: green: MWA with a-priori WDZe-model, orange: MWA with a-priori BF21-model.

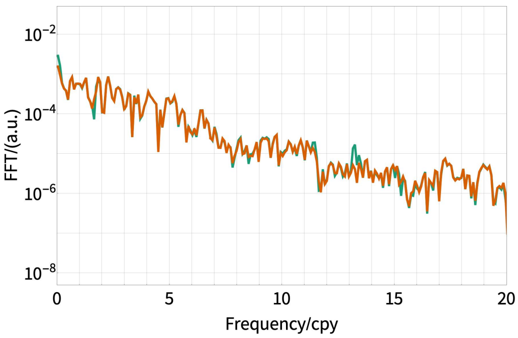

(a) Gravimetric factor of Q_1 tidal group

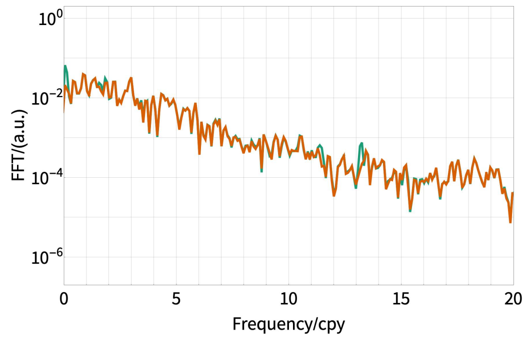

(b) Gravimetric phase of Q_1 tidal group

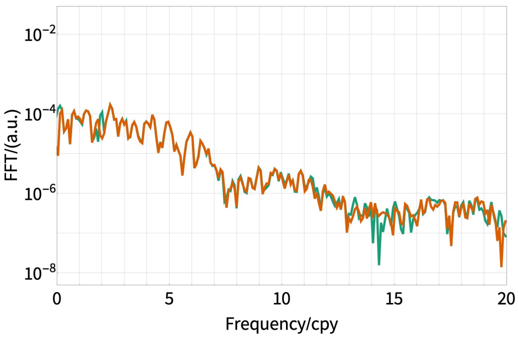

(c) Gravimetric factor of O_1 tidal group

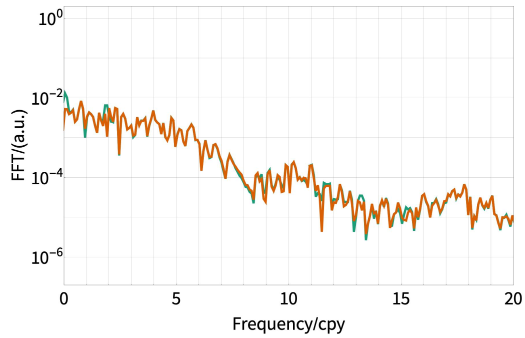

(d) Gravimetric phase of O_1 tidal group

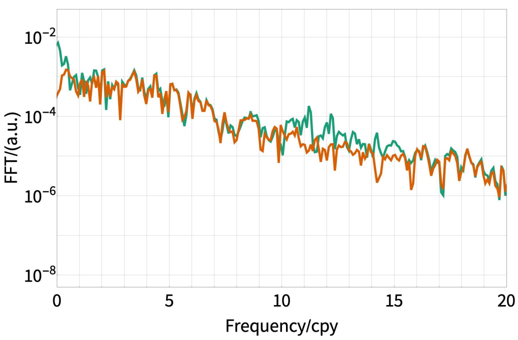

(e) Gravimetric factor of M_1 tidal group

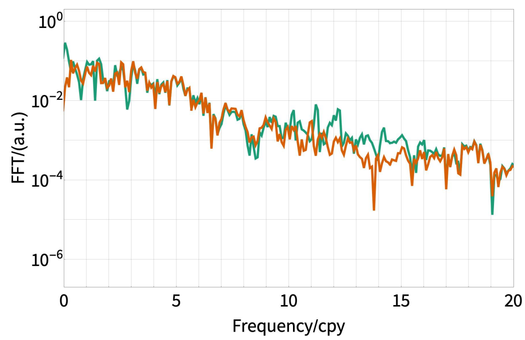

(f) Gravimetric phase of M_1 tidal group

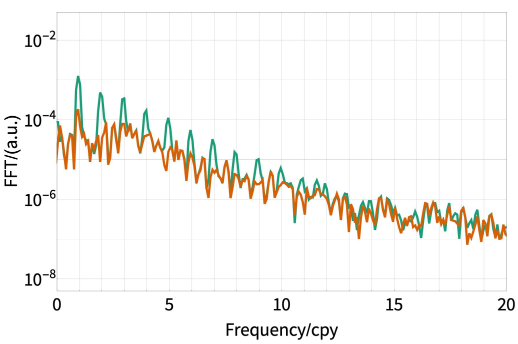

(g) Gravimetric factor of K_1 tidal group

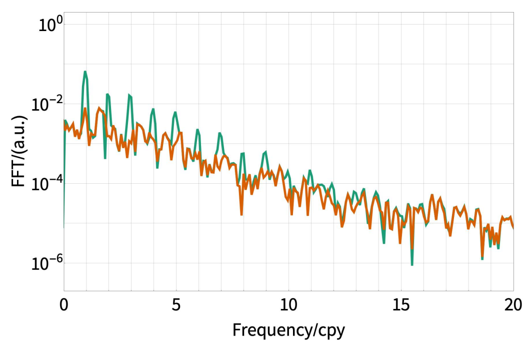

(h) Gravimetric phase of K_1 tidal group

Fig. S7: The spectra of moving window analysis for tidal groups Q_1, O_1, M_1 and K_1 (top to bottom) for gravimetric factor (left) and phase (right). Colors: green: MWA with a-priori WDZe-model, orange: MWA with a-priori BF21-model.

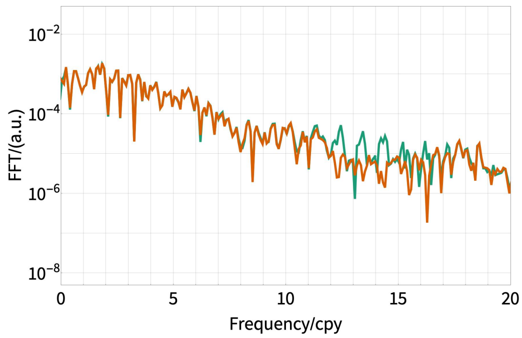

(a) Gravimetric factor of J_1 tidal group

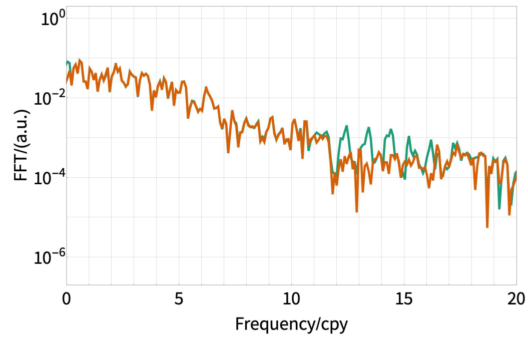

(b) Gravimetric phase of J_1 tidal group

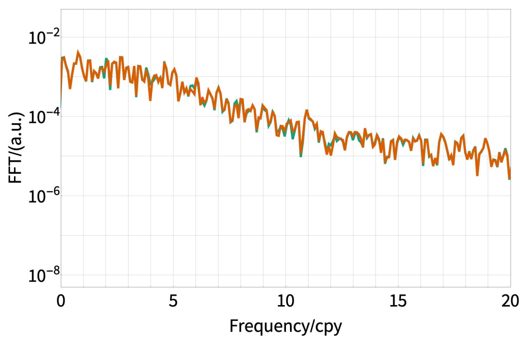

(c) Gravimetric factor of OO_1 tidal group

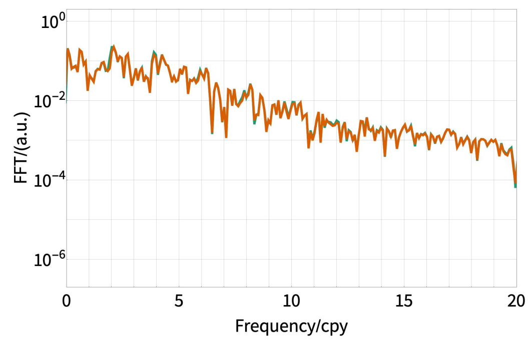

(d) Gravimetric phase of OO_1 tidal group

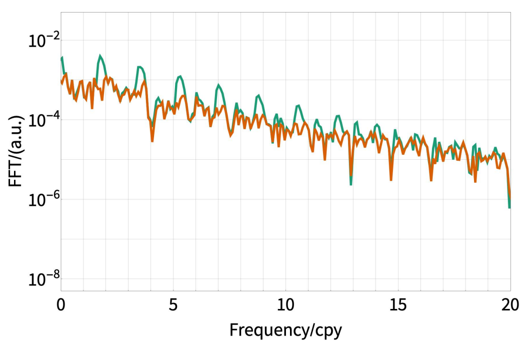

(e) Gravimetric factor of μ_2 tidal group

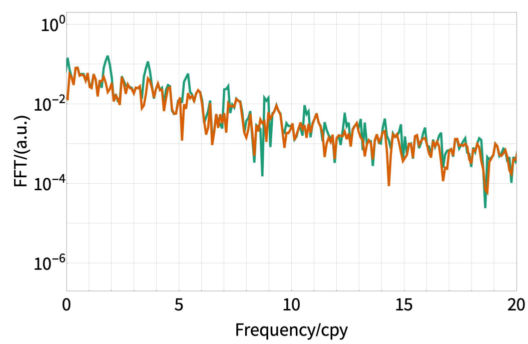

(f) Gravimetric phase of μ_2 tidal group

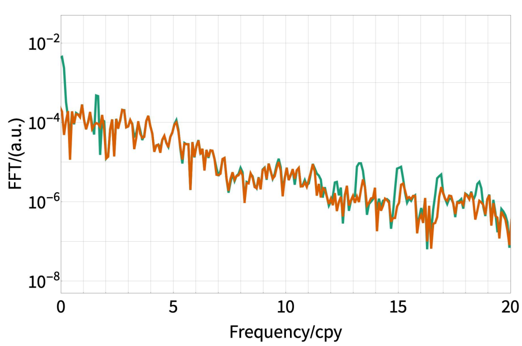

(g) Gravimetric factor of N_2 tidal group

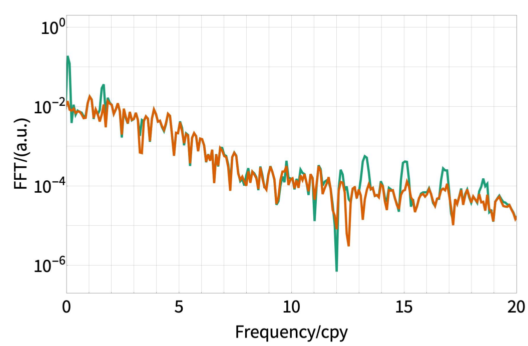

(h) Gravimetric phase of N_2 tidal group

Fig. S8: The spectra of moving window analysis for tidal groups J_1, OO_1, μ_2 and N_2 (top to bottom) for gravimetric factor (left) and phase (right). Colors: green: MWA with a-priori WDZe-model, orange: MWA with a-priori BF21-model.

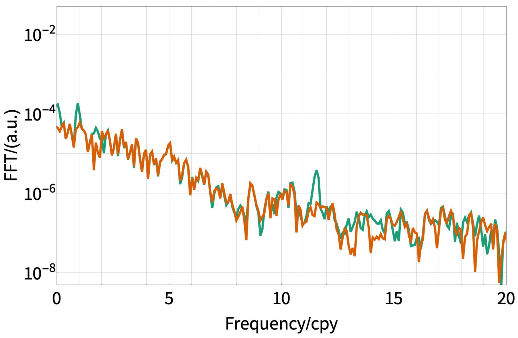

(a) Gravimetric factor of M_2 tidal group

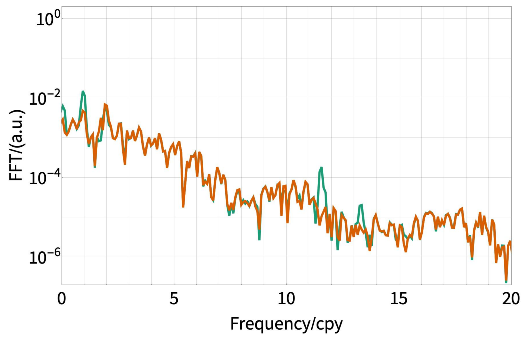

(b) Gravimetric phase of M_2 tidal group

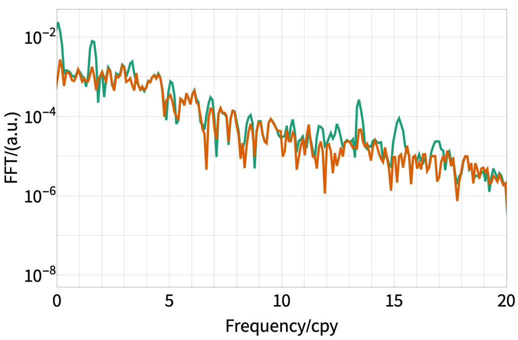

(c) Gravimetric factor of L_2 tidal group

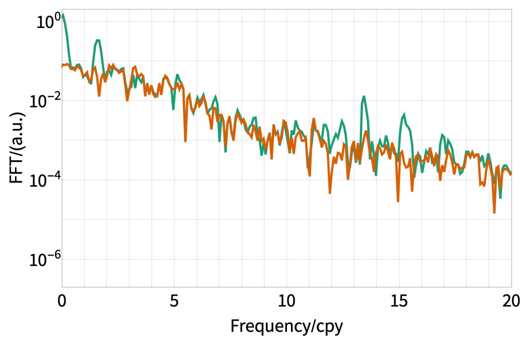

(d) Gravimetric phase of L_2 tidal group

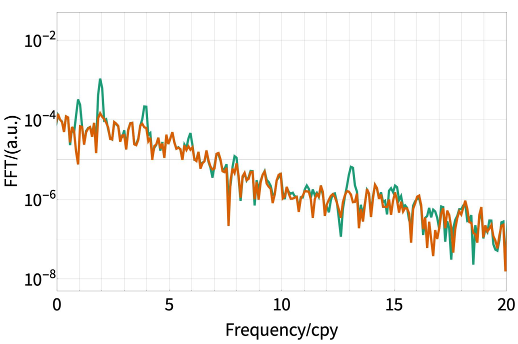

(e) Gravimetric factor of S_2 tidal group

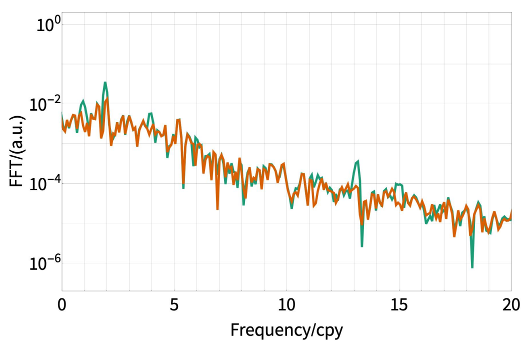

(f) Gravimetric phase of S_2 tidal group

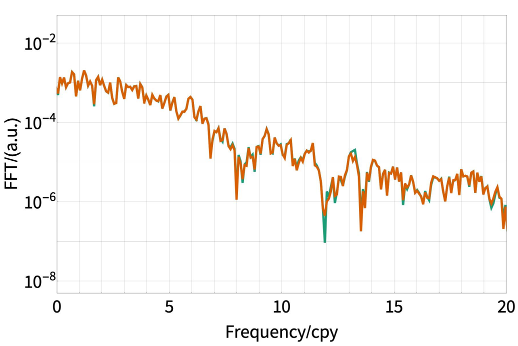

(g) Gravimetric factor of M_3* tidal group

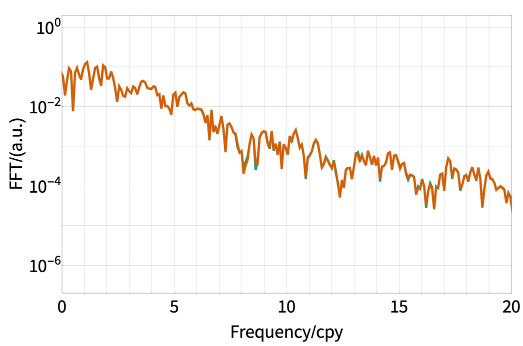

(h) Gravimetric phase of M_3* tidal group

Fig. S9: The spectra of moving window analysis for tidal groups M_2, L_2, S_2 and M_3* (top to bottom) for gravimetric factor (left) and phase (right). Colors: green: MWA with a-priori WDZe-model, orange: MWA with a-priori BF21-model.

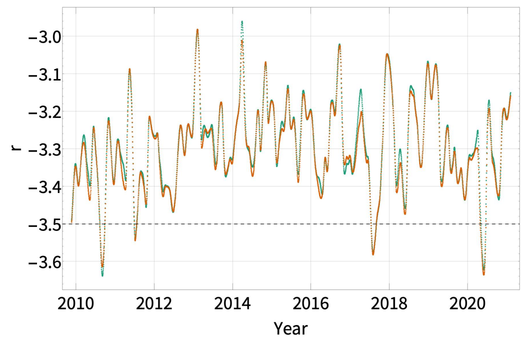

(a) Regression factor of air pressure

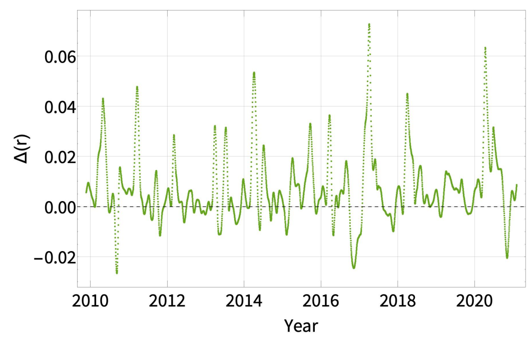

(b) Differences in air pressure regression factor.

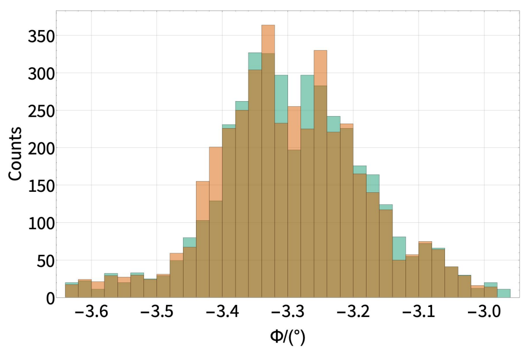

(c) Histogram of the coefficient for air pressure regression factor

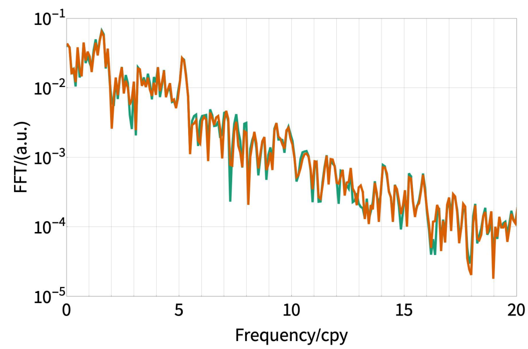

(d) Spectra of the coefficient for air pressure regression factor.

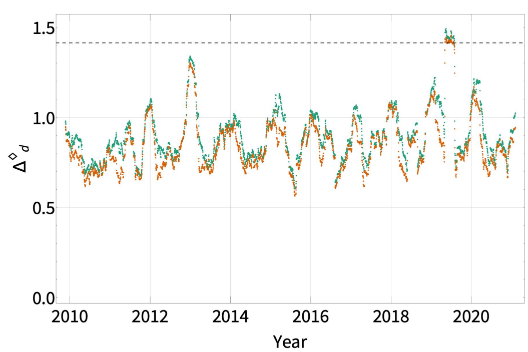

(e) Data misfit of untapered signals.

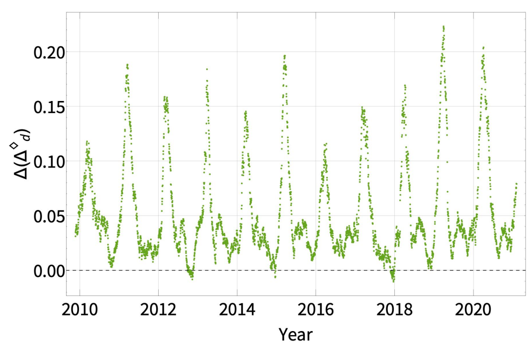

(f) Differences in data misfit of untapered signals.

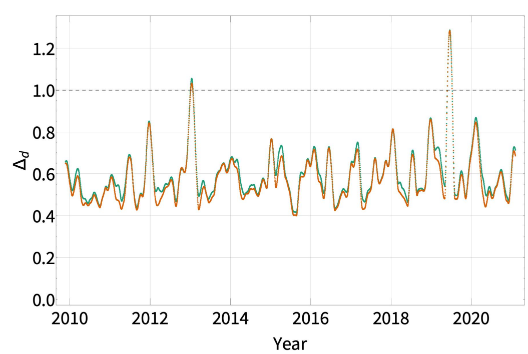

(g) Data misfit of tapered signals.

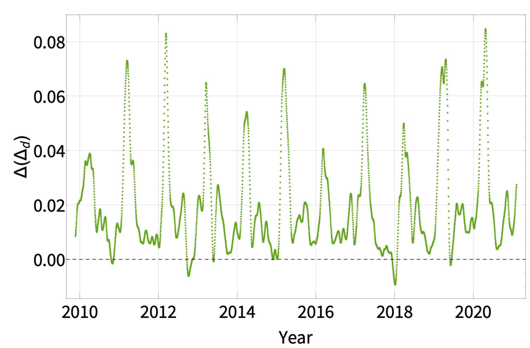

(h) Differences in data misfit of tapered signals.

Fig. S10: The moving window analysis: air pressure regression factor, its spectra and distribution; data misfit tapered and untapered. Colors: blue-green: MWA with a-priori WDZe-model, orange: MWA with a-priori BF21-model, green - differences between these two, WDZe-model - BF21-model.

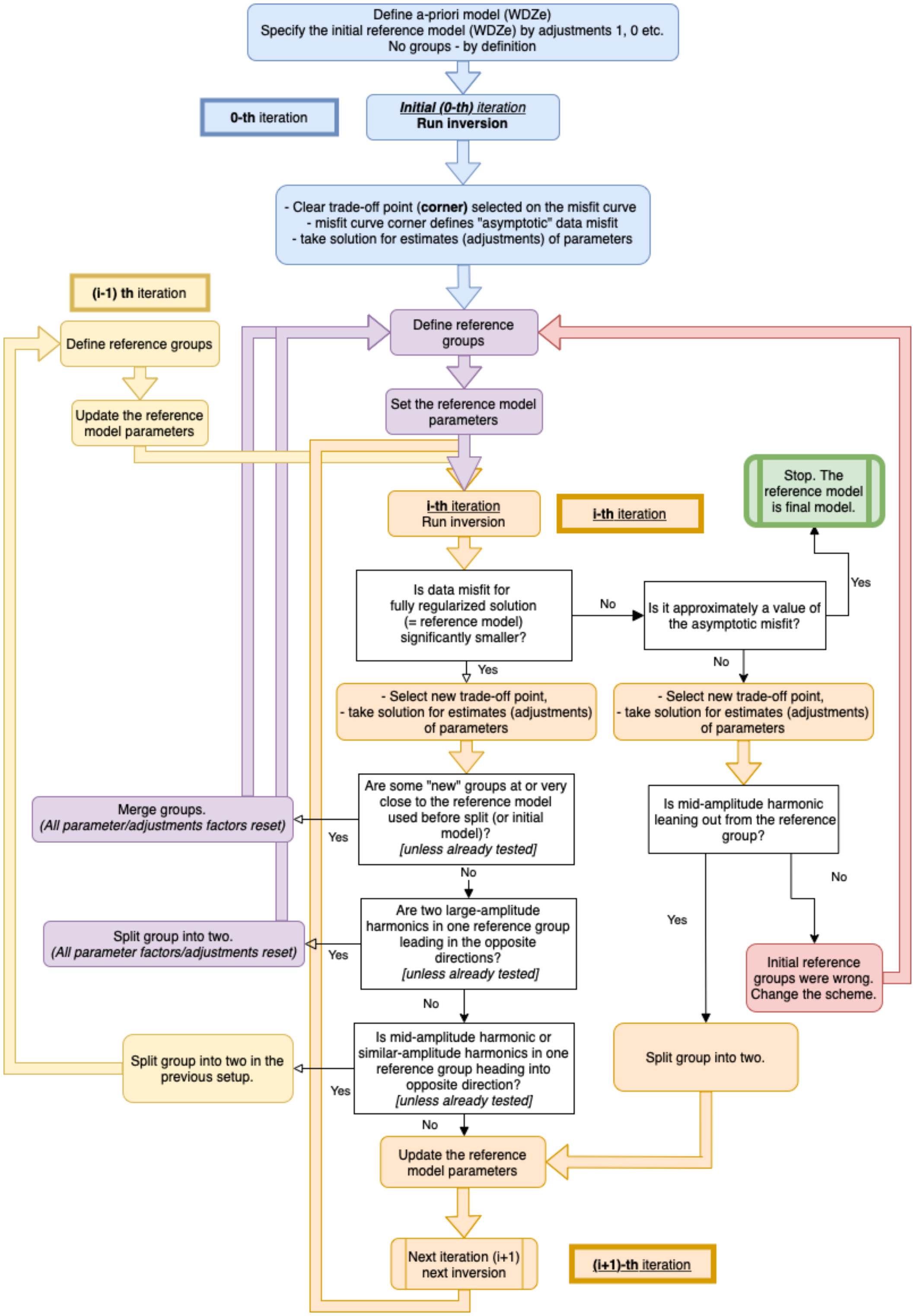

Fig. S11: Flowchart illustrating the RATA iteration procedure. Blue color represents the initial setup, that has to be performed only once within the workflow. White boxes are 'decision branches'. Items in orange are linear iterative paths. If the purple points are met, the parameters have to be reset to initial adjustments, but the reference group are modified only a little. Yellow track indiciates, that the last setup has to be altered. Red color is a clear information, that there was something wrong with our analysis. Green box is the end of the procedure. If we alter the grouping scheme, or reset the parameters, we keep information about the decisions (reference grouping, parameter update, etc.) that were made prior to that point.